

# Anagliptin Protected against Hypoxia/Reperfusion-Induced Brain Vascular Endothelial Permeability by Increasing ZO-1

Chuo Li,\* Yusheng Zhang, Rongrong Liu, and Yuzhen Mai



Cite This: *ACS Omega* 2021, 6, 7771–7777



Read Online

ACCESS |

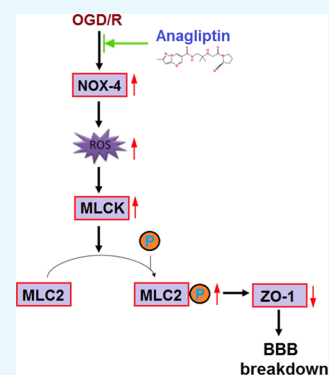


Metrics & More



Article Recommendations

**ABSTRACT:** Background and purpose: Cerebral ischemia-reperfusion injury is commonly induced during the treatment of ischemic stroke and is reported to be related to the blood–brain barrier destruction and brain vascular endothelial cell dysfunction. Anagliptin is a novel antidiabetic agent recently reported to protect neurons from oxidative stress. In the present study, we aim to investigate the protective property of anagliptin against oxygen–glucose deprivation and reperfusion (OGD/R)-induced injury on endothelial cells and clarify the potential underlying mechanism. Methods: OGD/R modeling was established on bEnd.3 brain endothelial cells. Cell viability was detected using the MTT assay, and the mitochondrial reactive oxygen species (ROS) level was measured using the mitoses red staining assay. The endothelial monolayer permeability was determined using an FITC-dextran permeation assay. The expression levels of NOX-4 and ZO-1 were evaluated using qRT-PCR and Western blot assays. The expressions of MLC-2, p-MLC-2, and myosin light chain kinase (MLCK) were determined using Western blot. Results: First, the decreased cell viability, upregulated NOX-4, and elevated mitochondrial ROS level in the endothelial cells induced by OGD/R were reversed by treatment with anagliptin. Second, the enlarged endothelial permeability and the decreased expression level of ZO-1 in the endothelial cells induced by OGD/R were alleviated by anagliptin. Third, the downregulation of ZO-1 and enlarged brain endothelial monolayer permeability induced by OGD/R were ameliorated by an MLCK inhibitor, ML-7. Lastly, the elevated expressions of MLCK and p-MLC-2 induced by OGD/R were suppressed by anagliptin. Conclusion: Anagliptin protected against hypoxia/reperfusion-induced brain vascular endothelial permeability by increasing the expression ZO-1, mediated by inhibition of the MLCK/MLC-2 signaling pathway.



## INTRODUCTION

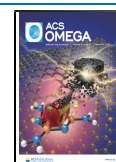
Ischemic stroke is a common clinical cerebrovascular disease with high morbidity. The rebuilding of the blood flow and the supply of blood and oxygen to ischemic areas are critical to the repairment of ischemic brain tissue injury. Accompanying the process of blood supply, reperfusion injury is regarded as a major concern.<sup>1</sup> Cerebral ischemia-reperfusion injury (CIRI) is defined as a clinical symptom of aggravation of the dysfunction of the brain metabolism and structural destruction induced by ischemia after restoring blood perfusion in ischemic brain tissues.<sup>2,3</sup> Therefore, in blood flow restoration for ischemic stroke treatment, it is important to ameliorate the destruction of the blood–brain barrier (BBB). The BBB is mainly composed of vascular endothelial cells, astrocytes, intercellular space, tight junction proteins, and basement membranes.<sup>4</sup> When CIRI occurs, a series of pathological changes are induced, including the production of free radicals, the overload of intracellular calcium, the disorder of energy metabolism, and neuron apoptosis, which contribute to endovascular edema, swollen astrocytes, breakage of basement membranes, and dissociation of intercellular junctions. As a consequence, the destruction of the BBB is induced.<sup>5,6</sup> The tight junction is a complex that mainly consists of transmembrane proteins, cytoplasmic accessory proteins, and cytoskeleton proteins,

which are indispensable to maintaining the integrity of the BBB and the core process of the pathophysiological changes of multiple nervous system diseases.<sup>7–10</sup> Zonula occludens-1 (ZO-1) plays an important role in connecting the transmembrane proteins and cytoskeletal proteins. The stability of the tight junction structure is impacted by the decreased expression level of ZO-1 or inactivation of ZO-1, regarded as one of the biomarkers of the destruction of the BBB.<sup>11</sup> Brain vascular endothelial cell dysfunction is also regarded as the pathological characteristic of the destruction of the BBB.<sup>12</sup> Brain vascular endothelial cells are the main location for the production of reactive oxygen species (ROS),<sup>13</sup> mediate oxidative stress, and contribute to the destruction of the BBB.<sup>14–16</sup> In addition, the myosin light chain kinase (MLCK)/MLC signaling pathway mediates the vascular permeability of brain vascular endothelial cells by regulating the expression of

Received: January 13, 2021

Accepted: February 22, 2021

Published: March 12, 2021



ACS Publications

© 2021 The Authors. Published by  
American Chemical Society

7771

<https://dx.doi.org/10.1021/acs.omega.1c00242>  
*ACS Omega* 2021, 6, 7771–7777

ZO-1<sup>17,18</sup> and is regulated by the excessively released ROS.<sup>19</sup> Therefore, reducing brain vascular endothelial permeability might be an effective target for the treatment of CIRI.

Anagliptin is an inhibitor of dipeptidyl peptidase IV (DPP-4) that was developed by Sanwa Kagaku Kenkyusho Co., Ltd and approved for the treatment of type II diabetes.<sup>20</sup> The molecular structure of anagliptin is shown in Figure 1.

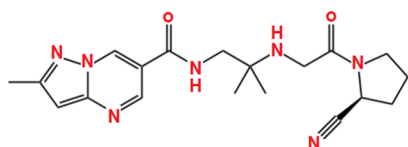


Figure 1. Molecular structure of anagliptin.

Anagliptin has shown promising antidiabetic properties in both clinical trials and animal experiments.<sup>21,22</sup> Recently, it was reported that the cytotoxicity and apoptosis induced by endogenous amyloid  $\beta$  in the neurons could be alleviated by anagliptin.<sup>23</sup> Pronounced antioxidative stress effects have also been reported during the treatment of type II diabetes with anagliptin.<sup>24</sup> In the present study, the protective effect of anagliptin against oxygen–glucose deprivation and reoxygenation (OGD/R)-induced injury on bEnd.3 brain endothelial cells will be investigated to explore the potential therapeutic property against CIRI.

## RESULTS

**Anagliptin Ameliorated OGD/R-Induced Reduction of Cell Viability in bEnd.3 Brain Endothelial Cells.** To investigate the protective effect of anagliptin against injury in bEnd.3 brain endothelial cells induced by OGD/R, bEnd.3 brain endothelial cells were exposed to OGD for 6 h, followed by reperfusion in normal culture media in the presence or absence of anagliptin (5 and 10  $\mu$ M) for 24 h. As shown in Figure 2A, clear and integrate morphology was observed in control bEnd.3 cells. The morphology of OGD/R-induced bEnd.3 cells was fuzzy and incomplete and significantly ameliorated by the introduction of anagliptin. The cell viability (Figure 2B) was also dramatically inhibited by OGD/R but greatly elevated by treatment with anagliptin in a dose-dependent manner. These data indicate that the cytotoxicity in bEnd.3 brain endothelial cells induced by OGD/R was ameliorated by anagliptin.

**Anagliptin Ameliorated OGD/R-Induced Expression of NOX-4 and the Production of Mitochondrial ROS in bEnd.3 Brain Endothelial Cells.** We further detected the state of oxidative stress in the treated bEnd.3 brain endothelial cells. As shown in Figure 3A,B, the elevated expression of NOX-4 induced by OGD/R was significantly suppressed by the introduction of anagliptin. The level of mitochondrial ROS was also significantly increased in OGD/R-treated bEnd.3 brain endothelial cells but pronouncedly inhibited by the administration of anagliptin in a dose-dependent manner. These data indicate that the oxidative stress in bEnd.3 brain endothelial cells induced by OGD/R was dramatically alleviated by anagliptin.

**Anagliptin Mitigates OGD/R-Induced Brain Endothelial Monolayer Permeability in bEnd.3 Brain Endothelial Cells.** To investigate the protective effect of anagliptin on the destructed BBB, the endothelial permeability of the monolayer consisting of treated bEnd.3 brain endothelial cells was

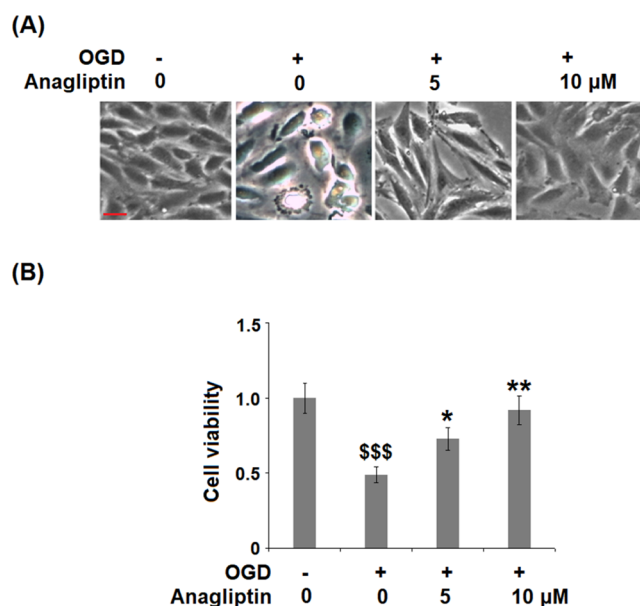


Figure 2. Anagliptin ameliorated OGD/R-induced reduction of cell viability in bEnd.3 brain endothelial cells. Cells were exposed to OGD for 6 h, followed by reperfusion in normal culture media in the presence or absence of anagliptin (5 and 10  $\mu$ M) for 24 h. (A) Morphology of bEnd.3 cells; scale bar, 50  $\mu$ m. (B) Cell viability measured using the MTT assay ( $n = 5$  or 6, \$\$\$,  $P < 0.005$  vs vehicle group; \*, \*\*,  $P < 0.05$ , 0.01 vs OGD/R group).

evaluated using an FITC-dextran permeation assay. As shown in Figure 4, compared to the control, the endothelial permeability was increased from 6.8 to 63.2% in the OGD/R-treated bEnd.3 cells but suppressed to 40.1 and 25.5% by treatment with anagliptin, respectively, indicating a protective effect of anagliptin against enlarged endothelial permeability induced by OGD/R.

**Anagliptin Ameliorated OGD/R-Induced Reduction of ZO-1 in bEnd.3 Brain Endothelial Cells.** ZO-1 is important in maintaining the integrity of the BBB. We further investigated the expression level of ZO-1 in the treated bEnd.3 cells. As shown in Figure 5, ZO-1 was found to be significantly downregulated in bEnd.3 cells by OGD/R but dramatically upregulated by the administration of anagliptin in a dose-dependent manner.

**Inhibition of MLCK with Its Inhibitor ML-7 Ameliorated Reduction of ZO-1 and Brain Endothelial Monolayer Permeability.** Cells were exposed to OGD for 6 h, followed by reperfusion in normal culture media in the presence or absence of ML-7 (10  $\mu$ M) for 24 h. As shown in Figure 6A, the expression of p-MLC-2 was significantly elevated in bEnd.3 cells by OGD/R but greatly suppressed by the introduction of ML-7, indicating an inhibitory effect of ML-7 against the MLCK/MLC-2 signaling pathway. The downregulated ZO-1 in OGD/R-treated bEnd.3 cells (Figure 6B,C) was greatly upregulated by treatment with ML-7. As shown in Figure 6D, compared to the control, the endothelial permeability was increased from 7.3 to 61.2% but suppressed to 19.6% by the introduction of ML-7. These data indicate that the reduction of ZO-1 and brain endothelial monolayer permeability induced by OGD/R were significantly ameliorated by blocking the MLCK/MLC-2 signaling pathway.

**Anagliptin Ameliorated OGD/R-Induced Expression of MLCK and p-MLC-2.** We further investigated the effects of

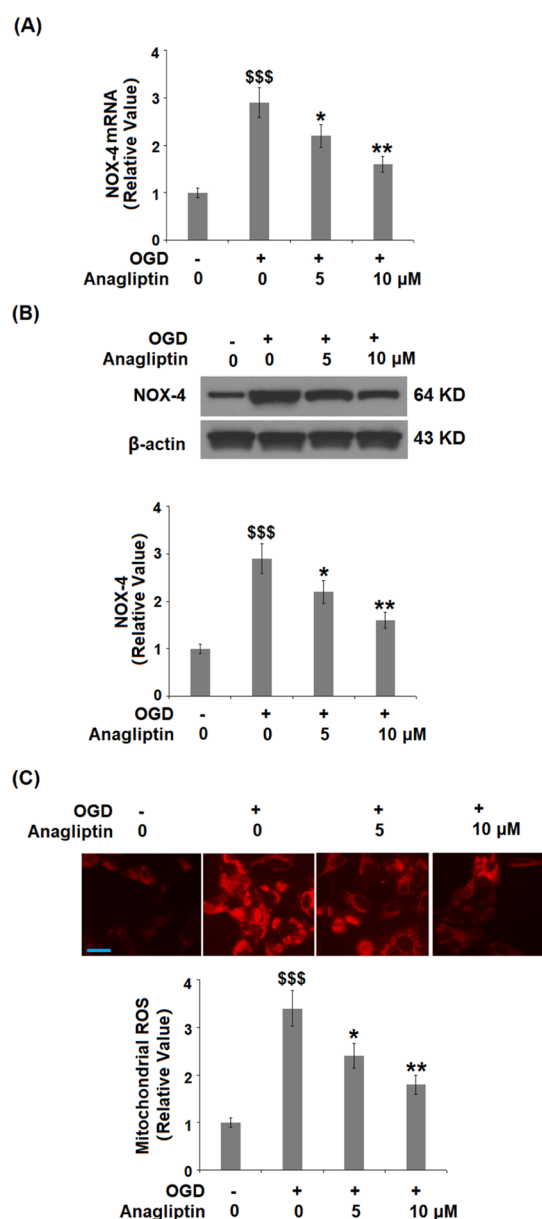


**Figure 3.** Anagliptin ameliorated OGD/R-induced expression of NOX-4 and the production of mitochondrial ROS in bEnd.3 brain endothelial cells. Cells were exposed to OGD for 6 h, followed by reperfusion in normal culture media in the presence or absence of anagliptin (5 and 10  $\mu$ M) for 24 h. (A) mRNA of NOX-4; (B) protein level of NOX-4; and (C) mitochondrial ROS measured using mitoxox red staining. Scale bar, 50  $\mu$ m ( $n = 5$ , \$\$\$,  $P < 0.005$  vs vehicle group; \*, \*\*,  $P < 0.05$ , 0.01 vs OGD/R group).

anagliptin on the MLCK/MLC-2 signaling pathway. Cells were exposed to OGD for 6 h, followed by reperfusion in normal culture media in the presence or absence of anagliptin (5 and 10  $\mu$ M) for 24 h. As shown in Figure 7A,B, the expression of MLCK was dramatically promoted in bEnd.3 cells by OGD/R but significantly suppressed by treatment with anagliptin. The upregulated p-MLC-2 in OGD/R-treated bEnd.3 cells was also greatly downregulated by the introduction of anagliptin in a dose-dependent manner. These data illustrate the inhibitory effect of anagliptin on the activated MLCK/MLC-2 signaling pathway induced by OGD/R.

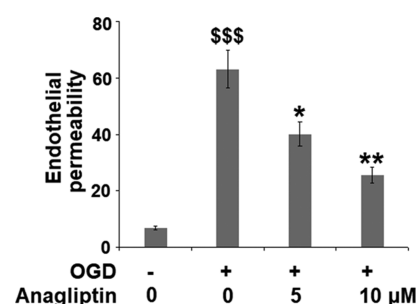


**Figure 4.** Anagliptin mitigates OGD/R-induced brain endothelial monolayer permeability in bEnd.3 brain endothelial cells. Cells were exposed to OGD for 6 h, followed by reperfusion in normal culture media in the presence or absence of anagliptin (5 and 10  $\mu$ M) for 24 h. Endothelial permeability was measured using FITC-dextran permeation ( $n = 6$ , \$\$\$,  $P < 0.005$  vs vehicle group; \*, \*\*,  $P < 0.05$ , 0.01 vs OGD/R group).

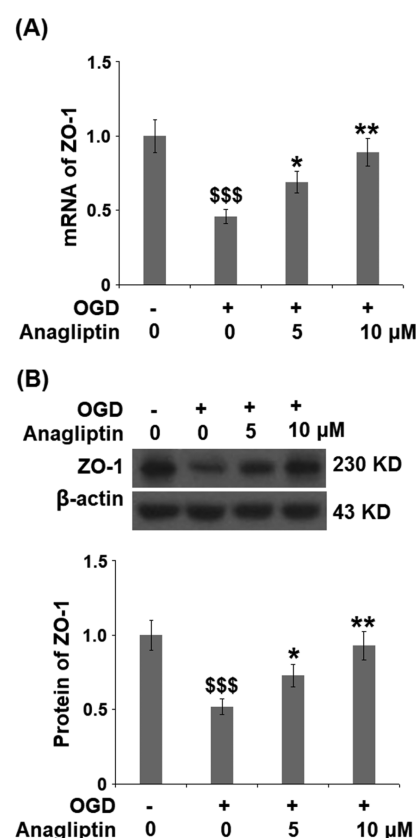


**Figure 5.** Anagliptin ameliorated OGD/R-induced reduction of ZO-1 in bEnd.3 brain endothelial cells. Cells were exposed to OGD for 6 h, followed by reperfusion in normal culture media in the presence or absence of anagliptin (5 and 10  $\mu$ M) for 24 h. (A) mRNA of ZO-1 and (B) protein of ZO-1 ( $n = 5$ , \$\$\$,  $P < 0.005$  vs vehicle group; \*, \*\*,  $P < 0.05$ , 0.01 vs OGD/R group).

## DISCUSSION

The production and metabolism of ROS in the endothelial cells are maintained by the balance between the oxidative and antioxidative systems under the normal physiological state and are essential for normal cellular function. However, under the CIRI state, excessive production of ROS is induced in endothelial cells, contributing to the activation of oxidative stress.<sup>25,26</sup> Oxidative stress induces endothelial cell dysfunction by releasing excessive superoxide, and the superoxide triggers

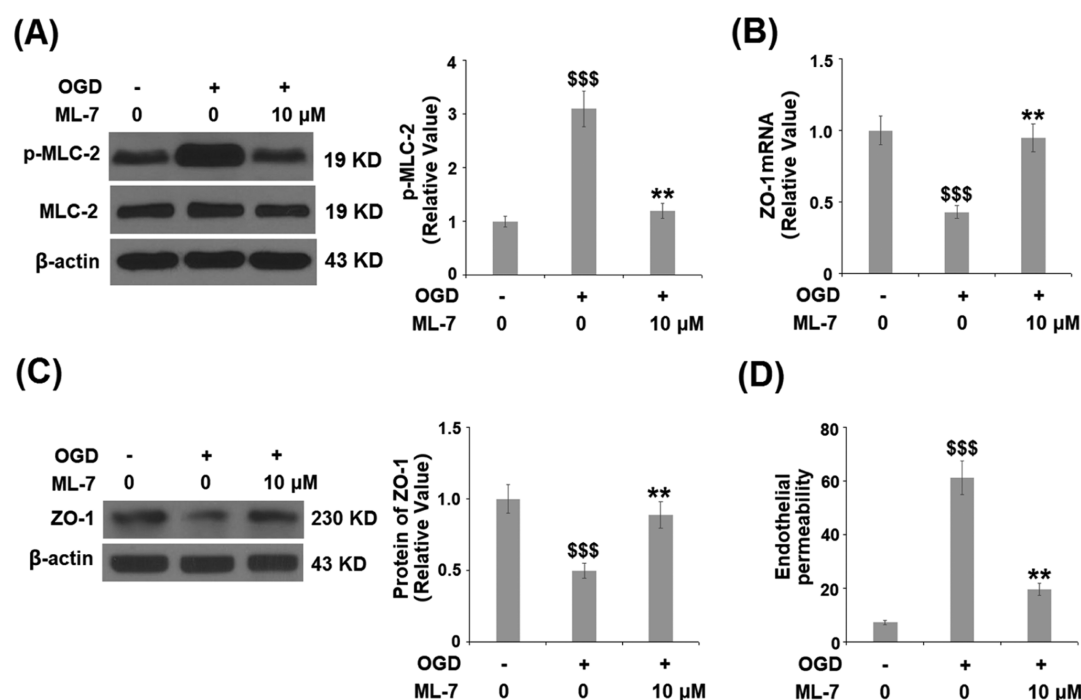


**Figure 6.** Inhibition of MLCK with its inhibitor ML-7 ameliorated reduction of ZO-1 and brain endothelial monolayer permeability. Cells were exposed to OGD for 6 h, followed by reperfusion in normal culture media in the presence or absence of ML-7 (10 μM) for 24 h. (A) Phosphorylated and total level of MLC-2; (B) mRNA of ZO-1; (C) protein level of ZO-1; and (D) endothelial permeability ( $n = 5$  or 6, \$\$\$,  $P < 0.005$  vs vehicle group; \*\*,  $P < 0.01$  vs OGD/R group).

the damages on bioactive substances, such as proteins, lipids, and DNAs, contributing to the apoptosis or death of endothelial cells.<sup>27</sup> In the present study, we found that the cytotoxicity in the brain endothelial cells induced by OGD/R was significantly ameliorated by treatment with anagliptin, indicating a promising protective effect of anagliptin on OGD/R-induced injury on brain endothelial cells. Further investigations revealed that the production of mitochondrial ROS induced by OGD/R was dramatically suppressed by anagliptin, indicating that the state of oxidative stress induced by OGD/R was alleviated by anagliptin. In addition, the expression of NADPH oxidase (NOX) 4, the main origin of ROS,<sup>28,29</sup> was downregulated by anagliptin, illustrating that the oxidative state in the OGD/R-treated brain endothelial cells was pronouncedly mitigated.

MLCK is a member of the calmodulin-dependent protein kinase family and plays an important role in regulating the permeability of vascular endothelia. MLC-2 is the main target of MLCK and mediates the actin contracts, as well as rearranges the distribution of cellular skeleton.<sup>30</sup> The MLCK signaling pathway regulates the structure of the cellular skeleton mainly by mediating the phosphorylation of MLC.<sup>31–33</sup> MLCK is an important protein kinase of p-MLC. The assembly of myosin II into myosin fibers is promoted, and the hydrolytic ATP is activated by the phosphorylation of MLC, stabilizing the interaction between myosin and actin and mediating the shrinkage of cytoskeletal microfilaments.<sup>34</sup> It is reported that centripetal retraction of myosin and actin filaments is induced by decreasing the concentration of extracellular calcium and the structure of tight junction is destroyed and can be blocked by the MLCK inhibitor or actin stabilizer.<sup>35</sup> Under pathological states, such as oxidative stress, the MLCK/MLC-2 signaling pathway is activated to mediate the constriction of actin, induce the remodeling of the cellular

skeleton, and destroy the intracellular tight junction, finally contributing to the permeability of endothelial.<sup>36</sup> In the present study, we found that the endothelial permeability was significantly enlarged by treatment with OGD/R but greatly alleviated by treatment with anagliptin, indicating a potential protective effect of anagliptin against the destroyed BBB. The injured tight junction between brain endothelial cells induced by OGD/R was also significantly repaired by anagliptin, which was verified by the upregulation of ZO-1, an important regulator of the tight junction.<sup>37</sup> We further validated that the damage of OGD/R against the tight junction and endothelial permeability could be ameliorated by ML-7, an inhibitor of MLCK, indicating that the MLCK/MLC-2 signaling pathway is involved in the pathogenesis of OGD/R-induced injury on endothelial cells. Lastly, we found that the MLCK/MLC-2 signaling pathway in the endothelial cells could be inhibited by anagliptin, indicating that the protective effect of anagliptin against OGD/R-induced injury on the endothelial cells might be related to the blockage of the MLCK/MLC-2 signaling pathway. However, the conclusion needed further verifications, such as introducing the activator MLCK/MLC-2 signaling pathway into the experimental system, which will be conducted in our future work. Furthermore, the therapeutic property of anagliptin against CIRI will be further verified by treating the middle cerebral artery occlusion animals, which will also be performed in our future work to confirm the therapeutic property of anagliptin.

Taken together, our data indicate that anagliptin protected against hypoxia/reperfusion-induced brain vascular endothelial injury *via* reduction of endothelial permeability through increasing the expression of ZO-1, mediated by the inhibition of the MLCK/MLC-2 signaling pathway.



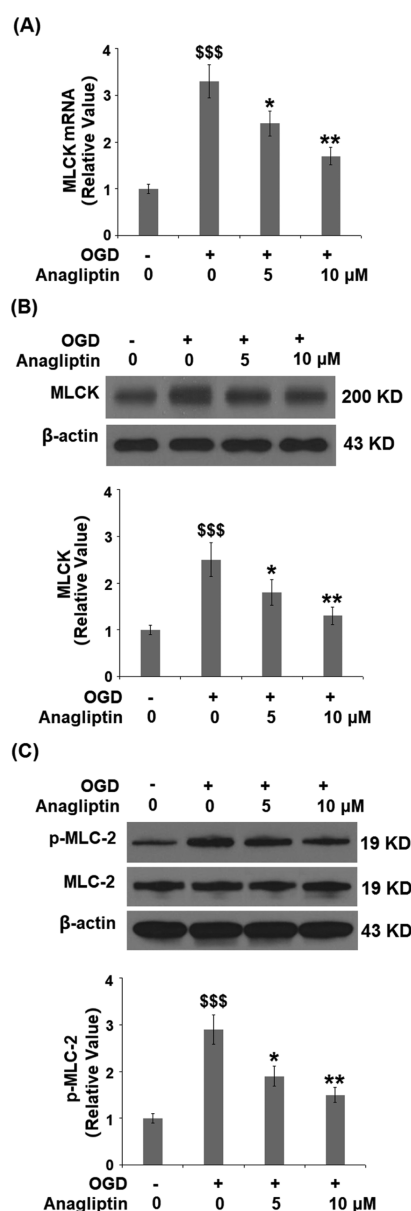


**Figure 7.** Anagliptin ameliorated OGD/R-induced expression of MLCK and phosphorylation of pMLC-2. Cells were exposed to OGD for 6 h, followed by reperfusion in normal culture media in the presence or absence of anagliptin (5 and 10  $\mu$ M) for 24 h. (A) mRNA of MLCK; (B) protein level of MLCK as measured by the Western blot analysis; and (C) level of phosphorylated and total level of MLC-2 ( $n = 5$  or 6, \$\$\$,  $P < 0.005$  vs vehicle group; \*, \*\*,  $P < 0.05$ , 0.01 vs OGD/R group).

## MATERIALS AND METHODS

**Cell Culture and Treatments.** The bEnd.3 brain endothelial cells were purchased from ATCC (Virginia, USA) and cultured in the complete DMEM medium (Thermo Fisher Scientific, Waltham, USA) containing 10% fetal bovine serum and 1% penicillin/streptomycin at 37 °C and CO<sub>2</sub>. The *in vitro* model of OGD/R was established according to the instruction described previously.<sup>38</sup> Briefly, for the OGD process, the cells were washed several times using the phosphate buffered saline (PBS) buffer and resuspended using the glucose-free DMEM medium. Subsequently, the bEnd.3 brain endothelial cells were transferred to a hypoxia chamber (containing a gas mixture of 5% CO<sub>2</sub> and 95% N<sub>2</sub>) at

37 °C to induce an OGD condition. Six hours later, the cells were returned to the normal incubator (95% air/5% CO<sub>2</sub>) in the presence or absence of anagliptin (5 and 10  $\mu$ M) for 24 h at 37 °C. Anagliptin (purity >98%) was commercially obtained from InvivoChem company (Cat#739366-20-2, China, Guangzhou).

**MTT Assay.** The viability of the treated bEnd.3 brain endothelial cells was evaluated using an MTT assay. In brief, the cells were planted on the 96-well plates and subjected to necessary treatment. After that, cells were loaded with 5 mg/mL MTT (Thermo, Massachusetts, USA) for 4 h. The reaction product was dissolved with dimethylsulfoxide. Lastly, absorbance at 490 nm was measured to index cell viability.

**MitoSox Red Staining.** MitoSox red assay was used to evaluate the production of mitochondrial ROS. Briefly, bEnd.3 brain endothelial cells were planted in the 24-well plates at a density of 50 000 cells/well, followed by being stained with 5  $\mu$ mol/L MitoSox-Red for 30 min in the dark at 37 °C. Subsequently, the cells were collected and washed using PBS buffer, and a fluorescent microscope was used to examine the red fluorescence.

**Real-Time PCR Assay.** RNAs from bEnd.3 cells were extracted using TRIzol (Cat#15596026, Invitrogen, USA), following the protocol for the product. The quantification of the total RNA was performed on a Nanodrop machine. RNA (2  $\mu$ g) was further reversely transcribed into cDNAs with the one-step cDNA Synthesis Kit (Bio-Rad, USA). Subsequently, the quantitative real-time PCR was performed using 2 $\times$  Power SYBR Green Master Mix (Invitrogen, California, USA). Finally, results were determined using the  $2^{-\Delta\Delta C_t}$  method. GAPDH was used as a housekeeping gene. The following primers were used in this study: ZO-1 (forward: 5'-AACTATGACCATCGC CATC-3', reverse: 5'-GCCTGTACCTGTTGTGCACC-3'); NOX4 (forward: 5'-TAG ATACCCACCCTCCCG-3', reverse: 5'-TGGGCTCTTCCATACAAATC-3'); MLCK (forward: 5'-CGCCACTTCCAGATAGACTAC-3', reverse: 5'-ACCTTCCTC CATCGTTTCC-3'); and GAPDH (forward: 5'-ATCAGCAATGCCTCCTGCAC-3', reverse: 5'-CGTCAA AGGTGGAGGAGTGG-3').

**Western Blot Assay.** Following lysing of the treated bEnd.3 brain endothelial cells using lysis buffer (Invitrogen, California, USA), the total proteins were extracted and quantified using the BCA kit (Beyotime Biotechnology, Shanghai, China). Subsequently, the proteins were loaded and separated using sodium dodecyl sulfate polyacrylamide gel electrophoresis, followed by being transferred to the PVDF membrane and incubated with 5% fat-free milk. The membranes were subsequently incubated with primary antibodies NOX-4 (1:2000, Cat#PA5-88106, Invitrogen, USA); ZO-1 (1:1000, Cat#5406, Cell Signaling Technology, USA); MLCK (1:2000, Cat#ab232949, Abcam, UK); MLC-2 (Cat#3672, Cell Signaling Technology, USA); p-MLC-2 (Cat#95777, Cell Signaling Technology, USA); and  $\beta$ -actin (1:5000, Cat#sc-47778, Santa Cruz Biotechnology, USA) and further incubated with a horseradish peroxidase-conjugated secondary antibody (1:1000, Cell Signaling Technology, USA) at room temperature for 1.5 h. Finally, the blots were incubated with ECL reagents (Thermo Fisher Scientific, USA) and visualized using ImageJ software.

**FITC-Dextran Permeation Assay.** FITC-dextran permeation assay was performed as previously described.<sup>39</sup> The monolayers were cultured using the treated bEnd.3 brain

endothelial cells at a density of  $2 \times 10^5$  cells/cm<sup>2</sup>. Subsequently, 500 µg/mL fluorescein isothiocyanate FITC-dextran was added to the apical compartment of the chamber, and samples (200 µL) from the basal medium (lower chamber) were collected 120 min after the addition of FITC-dextran. Finally, the absorbance of basal and apical medium samples was detected using a microplate reader (SpectraMax Gemini, California, USA) at 485 nm of excitation and 528 nm of emission.

**Statistical Analysis.** Experiments were repeated three times. All data were expressed as mean  $\pm$  SD. The data were analyzed using analysis of variance (ANOVA), followed by Dunnett's post hoc test for multiple comparisons, using Graph Pad Prism 6.0 (Graph Pad Software, La Jolla, CA, USA). Differences were considered significant with a *P*-value of less than 0.05.

## AUTHOR INFORMATION

### Corresponding Author

Chuo Li – Department of Neurology, Guangzhou Eighth People's Hospital of Guangzhou Medical University, Guangzhou, Guangdong 510440, China; [orcid.org/0000-0001-9318-8716](https://orcid.org/0000-0001-9318-8716); Phone: +86-020-36473145; Email: [lichuo2030@163.com](mailto:lichuo2030@163.com)

### Authors

Yusheng Zhang – Department of Neurology and Stroke Center, The First Affiliated Hospital of Jinan University, Guangzhou, Guangdong 510632, China

Rongrong Liu – Department of Neurology and Stroke Center, The First Affiliated Hospital of Jinan University, Guangzhou, Guangdong 510632, China

Yuzhen Mai – Department of Neurology, Guangzhou Eighth People's Hospital of Guangzhou Medical University, Guangzhou, Guangdong 510440, China

Complete contact information is available at:

<https://pubs.acs.org/10.1021/acsomega.1c00242>

### Notes

The authors declare no competing financial interest.

## ACKNOWLEDGMENTS

All supplements were supplied by Guangzhou Eighth People's Hospital of Guangzhou Medical University.

## REFERENCES

- (1) Zhang, H.; Park, J. H.; Maharjan, S.; Park, J. A.; Choi, K. S.; Park, H.; Jeong, Y.; Ahn, J. H.; Kim, I. H.; Lee, J. C.; Cho, J. H.; Lee, I. K.; Lee, C. H.; Hwang, I. K.; Kim, Y. M.; Suh, Y. G.; Won, M. H.; Kwon, Y. G. Sac-1004, a vascular leakage blocker, reduces cerebral ischemia-reperfusion injury by suppressing blood-brain barrier disruption and inflammation. *J. Neuroinflammation* **2017**, *14*, 122.
- (2) Liao, S.; Apaijai, N.; Chattipakorn, N.; Chattipakorn, S. C. The possible roles of necroptosis during cerebral ischemia and ischemia / reperfusion injury. *Arch. Biochem. Biophys.* **2020**, *695*, 108629.
- (3) Stegner, D.; Klaus, V.; Nieswandt, B. Platelets as Modulators of Cerebral Ischemia/Reperfusion Injury. *Front. Immunol.* **2019**, *10*, 2505.
- (4) Haaning, N.; Damsgaard, E. M.; Moos, T. The blood-brain barrier in ageing persons. *Ugeskr. Laeg.* **2018**, *180*, V08170576.
- (5) Lin, L.; Wang, X. Ischemia-reperfusion Injury in the Brain: Mechanisms and Potential Therapeutic Strategies. *Biochem. Pharmacol.* **2016**, *5*, 213.
- (6) Gong, P.; Li, R.; Jia, H.-Y.; Ma, Z.; Li, X.-Y.; Dai, X.-r.; Luo, S.-Y. Anfibatide Preserves Blood-Brain Barrier Integrity by Inhibiting TLR4/RhoA/ROCK Pathway After Cerebral Ischemia/Reperfusion Injury in Rat. *J. Mol. Neurosci.* **2020**, *70*, 71–83.
- (7) He, Q.; Liu, J.; Liang, J.; Liu, X.; Li, W.; Liu, Z.; Ding, Z.; Tuo, D. Towards Improvements for Penetrating the Blood-Brain Barrier-Recent Progress from a Material and Pharmaceutical Perspective. *Cells* **2018**, *7*, 24.
- (8) Lin, R.; Lang, M.; Heinsinger, N.; Stricsek, G.; Zhang, J.; Iozzo, R.; Rosenwasser, R.; Iacovitti, L. Stepwise impairment of neural stem cell proliferation and neurogenesis concomitant with disruption of blood-brain barrier in recurrent ischemic stroke. *Neurobiol. Dis.* **2018**, *115*, 49–58.
- (9) Kamei, N.; Yamaoka, A.; Fukuyama, Y.; Itokazu, R.; Takeda-Morishita, M. Noncovalent Strategy with Cell-Penetrating Peptides to Facilitate the Brain Delivery of Insulin through the Blood-Brain Barrier. *Biol. Pharm. Bull.* **2018**, *41*, 546–554.
- (10) Sonoda, H.; Morimoto, H.; Yoden, E.; Koshimura, Y.; Kinoshita, M.; Golovina, G.; Takagi, H.; Yamamoto, R.; Minami, K.; Mizoguchi, A.; Tachibana, K.; Hirato, T.; Takahashi, K. A Blood-Brain-Barrier-Penetrating Anti-human Transferrin Receptor Antibody Fusion Protein for Neuronopathic Mucopolysaccharidosis II. *Mol. Ther.* **2018**, *26*, 1366–1374.
- (11) Ma, J.; Wang, P.; Liu, Y.; Zhao, L.; Li, Z.; Xue, Y. Kruppel-like factor 4 regulates blood-tumor barrier permeability via ZO-1, occludin and claudin-5. *J. Cell. Physiol.* **2014**, *229*, 916–926.
- (12) Blanchette, M.; Daneman, R. Formation and maintenance of the BBB. *Mech. Dev.* **2015**, *138*, 8–16.
- (13) Fraser, P. A. The role of free radical generation in increasing cerebrovascular permeability. *Free Radical Biol. Med.* **2011**, *51*, 967–977.
- (14) Nito, C.; Kamada, H.; Endo, H.; Niizuma, K.; Myer, D. J.; Chan, P. H. Role of the p38 mitogen-activated protein kinase/cytosolic phospholipase A2 signaling pathway in blood-brain barrier disruption after focal cerebral ischemia and reperfusion. *J. Cereb. Blood Flow Metab.* **2008**, *28*, 1686–1696.
- (15) Betzen, C.; White, R.; Zehendner, C. M.; Pietrowski, E.; Bender, B.; Luhmann, H. J.; Kuhlmann, C. R. W. Oxidative stress upregulates the NMDA receptor on cerebrovascular endothelium. *Free Radical Biol. Med.* **2009**, *47*, 1212–1220.
- (16) Kishimoto, K.; Li, R. C.; Zhang, J.; Klaus, J. A.; Kibler, K. K.; Dore, S.; Koehler, R. C.; Sapirstein, A. Cytosolic phospholipase A2 alpha amplifies early cyclooxygenase-2 expression, oxidative stress and MAP kinase phosphorylation after cerebral ischemia in mice. *J. Neuroinflammation* **2010**, *7*, 42.
- (17) Huang, Y.; Luo, X.; Li, X.; Song, X.; Wei, L.; Li, Z.; You, Q.; Guo, Q.; Lu, N. Wogonin inhibits LPS-induced vascular permeability via suppressing MLCK/MLC pathway. *Vasc. Pharmacol.* **2015**, *72*, 43–52.
- (18) Ye, X.; Sun, M. AGR2 ameliorates tumor necrosis factor-alpha-induced epithelial barrier dysfunction via suppression of NF-kappaB p65-mediated MLCK/p-MLC pathway activation. *Int. J. Mol. Med.* **2017**, *39*, 1206–1214.
- (19) Rodrigues, S. F.; Granger, D. N. Blood cells and endothelial barrier function. *Tissue Barriers* **2015**, *3*, No. e978720.
- (20) Onoue, T.; Goto, M.; Wada, E.; Furukawa, M.; Okuji, T.; Okada, N.; Kobayashi, T.; Iwama, S.; Sugiyama, M.; Tsunekawa, T.; Takagi, H.; Hagiwara, D.; Ito, Y.; Morishita, Y.; Seino, Y.; Suga, H.; Banno, R.; Hamada, Y.; Ando, M.; Yamamori, E.; Arima, H. Dipeptidyl peptidase-4 inhibitor anagliptin reduces fasting apolipoprotein B-48 levels in patients with type 2 diabetes: A randomized controlled trial. *PLoS One* **2020**, *15*, No. e0228004.
- (21) Kawakubo, M.; Tanaka, M.; Ochi, K.; Watanabe, A.; Saka-Tanaka, M.; Kanamori, Y.; Yoshioka, N.; Yamashita, S.; Goto, M.; Itoh, M.; Shirakawa, I.; Kanai, S.; Suzuki, H.; Sawada, M.; Ito, A.; Ishigami, M.; Fujishiro, M.; Arima, H.; Ogawa, Y.; Suganami, T. Dipeptidyl peptidase-4 inhibition prevents nonalcoholic steatohepatitis-associated liver fibrosis and tumor development in mice independently of its anti-diabetic effects. *Sci. Rep.* **2020**, *10*, 983.

- (22) Kohno, D.; Furusawa, K.; Kitamura, T. Anagliptin suppresses diet-induced obesity through enhancing leptin sensitivity and ameliorating hyperphagia in high-fat high-sucrose diet fed mice. *Endocr. J.* **2020**, *67*, 523–529.
- (23) Chen, Z.; Tao, S.; Li, X.; Zeng, X.; Zhang, M.; Yao, Q. Anagliptin protects neuronal cells against endogenous amyloid beta (A $\beta$ )-induced cytotoxicity and apoptosis. *Artif. Cells, Nanomed., Biotechnol.* **2019**, *47*, 2213–2220.
- (24) Kakuda, H.; Kobayashi, J.; Kakuda, M.; Yamakawa, J.; Takekoshi, N. The effect of anagliptin treatment on glucose metabolism and lipid metabolism, and oxidative stress in fasting and postprandial states using a test meal in Japanese men with type 2 diabetes. *Endocrine* **2015**, *48*, 1005–1009.
- (25) Minutoli, L.; Puzzolo, D.; Rinaldi, M.; Irrera, N.; Marini, H.; Arcoraci, V.; Bitto, A.; Crea, G.; Pisani, A.; Squadrito, F.; Trichilo, V.; Bruschetta, D.; Micali, A.; Altavilla, D. ROS-Mediated NLRP3 Inflammasome Activation in Brain, Heart, Kidney, and Testis Ischemia/Reperfusion Injury. *Oxid. Med. Cell. Longevity* **2016**, *2016*, 2183026.
- (26) Jianrong, S.; Zhao, Y.; Yu, C.; Xu, J. DUSP14 rescues cerebral ischemia/reperfusion (IR) injury by reducing inflammation and apoptosis via the activation of Nrf-2. *Biochem. Biophys. Res. Commun.* **2019**, *509*, 713–721.
- (27) Liang, Y.; Li, J.; Lin, Q.; Huang, P.; Zhang, L.; Wu, W.; Ma, Y. Research Progress on Signaling Pathway-Associated Oxidative Stress in Endothelial Cells. *Oxid. Med. Cell. Longevity* **2017**, *2017*, 7156941.
- (28) Ikeda, R.; Ishii, K.; Hoshikawa, Y.; Azumi, J.; Arakaki, Y.; Yasui, T.; Matsuura, S.; Matsumi, Y.; Kono, Y.; Mizuta, Y.; Kurimasa, A.; Hisatome, I.; Friedman, S. L.; Kawasaki, H.; Shiota, G. Reactive oxygen species and NADPH oxidase 4 induced by transforming growth factor  $\beta$ 1 are the therapeutic targets of polyenylphosphatidylcholine in the suppression of human hepatic stellate cell activation. *Inflammation Res.* **2011**, *60*, 597–604.
- (29) He, W.; Shi, F.; Zhou, Z. W.; Li, B.; Zhang, K.; Zhang, X.; Ouyang, C.; Zhou, S. F.; Zhu, X. A bioinformatic and mechanistic study elicits the antifibrotic effect of ursolic acid through the attenuation of oxidative stress with the involvement of ERK, PI3K/Akt, and p38 MAPK signaling pathways in human hepatic stellate cells and rat liver. *Drug Des., Dev. Ther.* **2015**, *9*, 3989–4104.
- (30) Ye, S.; Song, Z.; Li, J.; Li, C.; Yang, J.; Chang, B. Early Intervention of Didang Decoction on MLCK Signaling Pathways in Vascular Endothelial Cells of Type 2 Diabetic Rats. *Int. J. Endocrinol.* **2016**, *2016*, 6704851.
- (31) Ivanov, A. I.; McCall, I. C.; Parkos, C. A.; Nusrat, A. Role for actin filament turnover and a myosin II motor in cytoskeleton-driven disassembly of the epithelial apical junctional complex. *Mol. Biol. Cell* **2004**, *15*, 2639–2651.
- (32) Shen, L.; Black, E. D.; Witkowski, E. D.; Lencer, W. I.; Guerriero, V.; Schneeberger, E. E.; Turner, J. R. Myosin light chain phosphorylation regulates barrier function by remodeling tight junction structure. *J. Cell Sci.* **2006**, *119*, 2095–2106.
- (33) Hecht, G.; Pestic, L.; Nikcevic, G.; Koutsouris, A.; Tripuraneni, J.; Lorimer, D. D.; Nowak, G.; Guerriero, V., Jr.; Elson, E. L.; Lanerolle, P. D. Expression of the catalytic domain of myosin light chain kinase increases paracellular permeability. *Am. J. Physiol.* **1996**, *271*, C1678–C1684.
- (34) Suzuki, K.; Takahashi, K. Actin filament assembly and actin-myosin contractility are necessary for anchorage- and EGF-dependent activation of phospholipase C $\gamma$ . *J. Cell. Physiol.* **2001**, *189*, 64–71.
- (35) Ma, T. Y.; Tran, D.; Hoa, N.; Nguyen, D.; Merryfield, M.; Tarnawski, A. Mechanism of extracellular calcium regulation of intestinal epithelial tight junction permeability: role of cytoskeletal involvement. *Microsc. Res. Tech.* **2000**, *51*, 156–168.
- (36) Tao, T.; Wang, X.; Liu, M.; Liu, X. Myofibrillogenesis regulator-1 attenuates hypoxia/reoxygenation-induced injury by repairing microfilaments in neonatal rat cardiomyocytes. *Exp. Cell Res.* **2015**, *337*, 234–242.
- (37) Schwyer, C.; Shamipour, S.; Pranjić-Ferscha, K.; Schauer, A.; Balda, M.; Tada, M.; Matter, K.; Heisenberg, C.-P. Mechanosensation of Tight Junctions Depends on ZO-1 Phase Separation and Flow. *Cell* **2019**, *179*, 937–952.
- (38) Liu, X.; Ma, Y.; Wei, X.; Fan, T. Neuroprotective effect of licochalcone A against oxygen-glucose deprivation/reperfusion in rat primary cortical neurons by attenuating oxidative stress injury and inflammatory response via the SIRT1/Nrf2 pathway. *J. Cell. Biochem.* **2018**, *119*, 3210–3219.
- (39) Suzuki, K.; Koyanagi-Aoi, M.; Uehara, K.; Hinata, N.; Fujisawa, M.; Aoi, T. Directed differentiation of human induced pluripotent stem cells into mature stratified bladder urothelium. *Sci. Rep.* **2019**, *9*, 10506.